(This is a sample cover image for this issue. The actual cover is not yet available at this time.)

FEBS Open Bio 2 (2012) 305–312

FEBS openbio

journal homepage: www.elsevier.com/locate/febsopenbio

Nitric oxide, substrate of *Euphorbia characias* peroxidase, switches off the CN^- inhibitory effect

Francesca Pintus[a], Delia Spanò[a], Andrea Bellelli[b], Francesco Angelucci[c], Elena Forte[b], Rosaria Medda[a], Giovanni Floris[a,*]

[a] Department of Sciences of Life and Environment, University of Cagliari, I-09042 Monserrato, Cagliari, Italy
[b] Department of Biochemical Sciences "A. Rossi Fanelli", University of Rome "La Sapienza" and CNR Institute of Molecular Biology and Pathology, I-00185 Rome, Italy
[c] Department of Life, Health and Environmental Sciences, University of l'Aquila, I-67100 L'Aquila, Italy

ARTICLE INFO

Article history:
Received 8 August 2012
Received in revised form 10 September 2012
Accepted 23 September 2012

Keywords:
Nitric oxide
Cyanide
Peroxidase
Latex
Euphorbia characias

ABSTRACT

The oxidation of nitric oxide (NO) by *Euphorbia characias* latex peroxidase (ELP-Fe^{III}), in the presence or in the absence of added calcium, has been investigated. The addition of hydrogen peroxide to the native enzyme leads to the formation of Compound I and serves to catalyse the NO oxidation. The addition of NO to Compound I leads to the formation of Compound II and, afterwards, to the native enzyme spectrum. Under anaerobic conditions, the incubation of the native enzyme (ELP-Fe^{III})with NO leads to the formation of the stable complex, showing a characteristic absorption spectrum (ELP-Fe^{II}–NO^+). The rate of the formation of this complex is slower in the presence of calcium than in its absence, and the same applies to the rate of the formation of Compound II from Compound I, using NO as substrate. Finally, we demonstrate that NO protects ELP from the inactivation caused by CN^- *via* a mechanism presumably requiring the formation of an enzyme-nitrosyl cyanide complex.

1. Introduction

The free radical nitric oxide (NO) is an ubiquitous signalling molecule involved in a large number of physiological processes. While in animals NO is produced from L-arginine by nitric oxide synthases or not enzymatically (but possible catalysed by globins) from nitrite, NO synthesis appears more complex in plants and it may be arginine-dependent or nitrite-dependent, this latter by enzymatic or non-enzymatic routes. Several original papers and reviews have been published in the last years concerning NO synthesis in plants and it is therefore difficult to quote them all. As examples, we can cite some of these ([1–4] and references therein).

An important aspect of NO-synthesis is the involvement of polyamines inducing the production of NO [5], and the presence of an unknown enzyme responsible for the direct conversion of polyamines to NO has been hypothesised [6].

Peroxidases (E.C. 1.11.1.x; donor: hydrogen peroxide oxidoreductase) are enzymes utilising hydrogen peroxide or other peroxides to oxidise a second reducing substrate. Heme containing peroxidases (E.C. 1.11.1.7) are grouped in major (super)families one of which is a catalase–peroxidase superfamily [7]. This latter group can be subdivided into three classes (I, II and III) on the basis of sequence similarity. Class III includes the secretory plant peroxidases, monomeric glycosylated proteins distributed throughout the plant kingdom [8,9]. These enzymes are implicated in several plant physiological processes, such as hydrogen peroxide detoxification, auxin metabolism, cell elongation, lignin and suberin formation, salt tolerance and oxidative stress. Moreover, when plants are attacked by pathogens, several defence mechanisms are activated and Class III peroxidases play a very special physiological role [10–12].

Two well studied examples of Class III peroxidases are the enzymes extracted from horseradish (HRP; [13] and references therein) and from latex of the perennial Mediterranean shrub *Euphorbia characias* (ELP; [14]). ELP is present in the latex as unique isoenzymatic form constituted by a single glycosylated polypeptide chain of 347 amino acid residues with a relative molecular mass of 47 kDa and contains a ferric iron-protoporphyrin IX pentacoordinated to a proximal histidine ligand. The ELP sequence ([15]; GenBank accession number AY586601) permits identification of two highly conserved histidine residues (His_{50} and His_{179}, distal and proximal, respectively). Alike other secreted plant peroxidases, ELP has two calcium binding sites namely "proximal" and "distal" but, unlike to these, the purified protein contains only one mol of endogenous Ca^{2+}/mol enzyme strongly bound to the proximal site. This proximal Ca^{2+} ion plays a critical role for retaining the active site geometry. A second Ca^{2+} ion, necessary for expression of the full activity of the enzyme, appears to be located

Abbreviations: ABTS, 2,2′-azinobis(3-ethylbenzthiazoline-6-sulphonic) acid; ELP-Fe^{III}, *Euphorbia* latex peroxidase; HRP, horseradish peroxidase

* Corresponding author. Address: Dipartimento di Scienze della Vita e dell'Ambiente, Cittadella Universitaria, I-09042 Monserrato, Cagliari,Italy. Tel.: +39 070 6754519; fax: +39 070 6754523.
E-mail address: florisg@unica.it (G. Floris).

2211-5463/$36.00
http://dx.doi.org/10.1016/j.fob.2012.09.004

at the distal low affinity binding site [16].

The kinetic mechanism of ELP is well established [14,17] and is briefly summarised here. The reaction of hydrogen peroxide with ELP ($PrIXFe^{III}$) generates the green enzyme intermediate Compound I ($PrIX^{\bullet+}Fe^{IV}=O$), with both of the oxidising equivalents of H_2O_2 transferred to the enzyme. One of the two oxidising equivalents of peroxide is accounted for by the loss of an electron from the iron atom that is oxidised to a ferryl complex in Compound I ($Fe^{IV}=O^{2-}$), whereas the second electron is donated by the porphyrin ring, oxidised to a π-cation radical. Compound I then reverts to the resting state by two successive one-electron reactions with reducing substrate molecules (AH_2). The red Compound II ($PrIXFe^{IV}=O$), a second enzyme intermediate, is produced by the first electron transfer from AH_2 to Compound I.

We previously reported that calcium ions enhance the catalytic efficiency of ELP toward substrates during the peroxidative cycle [14], reduce ELP activity in the so called catalase-like cycle [18], and regulate the ability of the enzyme to execute different metabolic pathways toward the same substrate, as in the oxidation of tyramine [19] and thiocyanate [20]. In this study we have investigated the binding and the oxidation of NO by *Euphorbia* peroxidase in the presence and absence of calcium ions. We show that native ELP forms, both in the absence or in the presence of calcium ions, a stable complex with nitric oxide but, in the presence of these ions, the affinity of ELP for NO is lowered by a factor of 3. Moreover, native ELP utilises NO as second substrate by an usual kinetic model to form Compound II from Compound I, and the native enzyme from Compound II. In the presence of calcium added, after addition of NO to Compound I, the Compound II is formed but evolves to a slow process that populates ELP-Fe^{II}–NO^+ complex. Finally, probably the most interesting and new result, we show that NO protects ELP from the inactivation caused by CN^- by a novel mechanism requiring the formation of an enzyme-nitrosyl cyanide complex.

2. Materials and methods

2.1. Materials

2,2′-Azinobis(3-ethylbenzthiazoline-6-sulphonic) acid (ABTS), guaiacol, ascorbic acid and diethylamine–NONOate (DEA/NO) were purchased from Sigma (St. Louis, MO). We used DEA/NO for the reliable generation of nitric oxide and we considered 16 min the half-life of DEA/NO (25 °C and pH 7.0) and 1.5 the efficiency of NO release (mol NO per mol that dissociates) [21]. Hydrogen peroxide was from Merck (Darmstadt, Germany) and an $\varepsilon_{240}=43.6\ M^{-1}\ cm^{-1}$ was used to determine its concentration. All reagents were obtained as pure commercial products and used without further purification.

2.2. Enzyme

Peroxidase from *E. characias* latex (Reinheitzahl (RZ) value $A_{401}/A_{278}=2.7$ in 100 mM Tris–HCl buffer, pH 7.0) was purified as previously described [14]. The enzyme concentration was determined spectrophotometrically using an $\varepsilon_{401}=130.7\ mM^{-1}\ cm^{-1}$.

2.3. Spectrophotometry

Absorption spectra and data from all activity assays were obtained with an Ultrospec 2100 spectrophotometer (Biochrom Ltd., Cambridge, England) using cells with a 1 cm path length.

Anaerobic experiments were made in a Thunberg-type spectrophotometer cuvette (Soffieria Vetro, Sassari, Italy) after several cycles of evacuation followed by flushing with O_2-free argon. Anaerobic additions of various reagents to the cuvette were made through a rubber cap with a syringe.

2.4. Peroxidase activity

Activity measurements were performed in 100 mM Tris–HCl buffer, pH 7.0, in both the absence and the presence of 10 mM Ca^{2+} ions, using hydrogen peroxide and the reducing substrate by the below reported procedures:

(i) ABTS oxidation following the increase in absorbance at 415 nm resulting from the formation of the ABTS cation radical product ($\varepsilon_{415}=36\ mM^{-1}\ cm^{-1}$).
(ii) Guaiacol following its oxidation by the increase in absorbance at 470 nm ($\varepsilon_{470}=26.6\ mM^{-1}\ cm^{-1}$ [22]).
(iii) NO oxidation by NO electrode (see below).

2.5. NO electrode

Stock solutions of NO (Air Liquide, Paris, France) were prepared by equilibrating degassed water at room temperature with the pure gas at 1 atm. NO measurements were carried out at 25 °C using a NO selective electrode (ISO-NO MarkII World Precision Instruments, Florida, USA). O_2 concentration in the assay was also monitored, in parallel, using a high resolution respirometer (Oxygraph-2k, Oroboros Instruments, Innsbruck, Austria). In a typical experiment, NO-equilibrated water was added to the reaction chamber of the respirometer ($V=1.5$ mL) containing deoxygenated and N_2-equilibrated 100 mM Tris–HCl buffer, pH 7.0. Afterwards, 1.5 μL of ELP (0.1 μM final) and H_2O_2 were added and the rise and fall in NO concentration was continuously monitored.

The value of K_m for ELP using varying NO concentrations (1–10 μM) at a fixed concentration of hydrogen peroxide (10 μM), or varying concentrations of hydrogen peroxide (0.1–5 μM) at a fixed concentration of NO (5 μM), was calculated from data fitted to the Michaelis–Menten equation by nonlinear regression and by double reciprocal plots by Michaelis–Menten analysis. Catalytic centre activity (k_{cat}) was defined as (mol of substrate consumed)/(mol of enzyme active sites) × s^{-1}. The k_{cat}/K_m value was also used as measure of substrate specificity. The effects of Ca^{2+} ions on ELP activity were examined in buffers with or without $CaCl_2$. All kinetic parameters were the mean of three different determinations.

2.6. Stopped-flow experiments

Stopped-flow experiments were carried out using an Applied Photophysics MV 17 apparatus (Leatherhead, UK), equipped with an observation chamber with a 1 cm path length and either a monochromator and a photomultiplier tube (for single wavelength measurements) or a spectrometer and a photodiode array detector (for rapid acquisition of absorbance spectra over the range 250–800 nm). Single wavelength measurements were analysed by a least squares minimisation routine (developed using the Borland Pascal 7.0 compiler) capable of fitting any desired theoretical model to the experimental data, using either analytical or numerical integration.

2.7. Laser photolysis experiments

Laser photolysis experiments were carried out using the instrument previously described ([23,24] and references therein). The instruments allowed different setups of which only one was used for the experiments described below. A pulsed Nd-YAG solid-state laser (model HIL 101, Quanta System, Milano, Italy) capable of 5 ns pulses of 80 mJ at $\lambda = 532$ nm, was focused onto an optical Thunberg tube containing the desired solution. The transmittance of the sample was monitored using the stationary light, orthogonal to the laser beam, emitted by a 50-W lamp. The observation wavelength (425 nm)

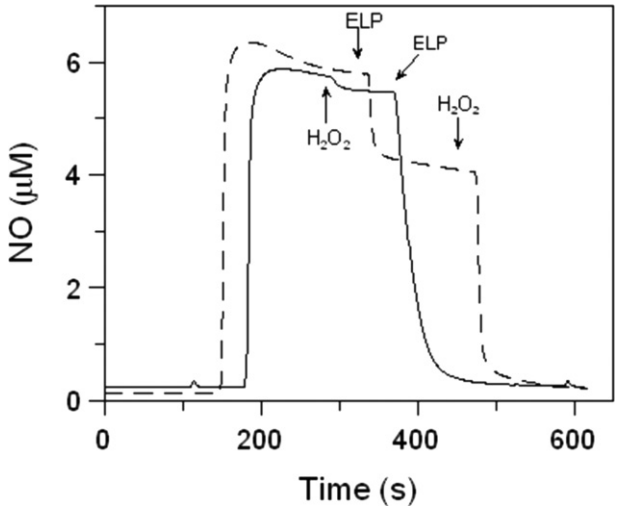

Fig. 1. Effect of ELP and hydrogen peroxide on NO consumption. Solid line: a typical trace recording in a chamber equipped with an NO-selective electrode showing the rapidly NO signal increase. Addition of hydrogen peroxide (500 μM) to the reaction mixture has no significant effect on the rate of NO consumption. The addition of ELP (0.1 μM) induces a rapid disappearance of NO. Dotted line: ELP (1.5 μM) binds NO causing a decrement in NO concentration. The addition of H_2O_2 results in the rapid consumption of NO. Buffer 100 mM Tris–HCl, pH 7.0.

was obtained using a Spex 1681 monochromator, and a Hamamatsu H6780-01 photosensor module was used to measure the transmitted light. The current emitted by the photosensor was amplified using a Hamamatsu C1053 current to voltage amplifier and read using a digital Tektronix TDS 360 oscilloscope.

3. Results

3.1. NO is a substrate for Euphorbia peroxidase

The addition of NO under anaerobic conditions to 100 mM Tris–HCl buffer, pH 7.0 (5 μM NO final), in a chamber equipped with a NO-selective electrode, showed that the NO signal increased rapidly (Fig. 1, solid line). Addition of hydrogen peroxide (500 μM) to the reaction mixture had no significant effect on the concentration of NO. Addition of ELP (0.1 μM) to the reaction mixture, induced a rapid disappearance of NO from solution clearly indicating that NO was rapidly and completely metabolised. The addition of ELP (1.5 μM) to the reaction mixture, in anaerobic conditions but without hydrogen peroxide, caused a protein-concentration dependent (approximately equimolar) decrement in NO concentration (Fig. 1, dotted line). The addition of H_2O_2 rapidly induced a disappearance of NO from solution, indicating again that NO was rapidly and completely metabolised.

The value of K_m for NO at high concentrations of hydrogen peroxide (10 μM) was shown to be 2 μM whereas the K_m for hydrogen peroxide at high concentrations of NO (5 μM) was calculated to be 1.6 μM (Table 1). Both K_m values appeared significantly lower than those observed with other substrates indicating a very high affinity of ELP for NO.

ELP showed a k_{cat} value and a k_{cat}/K_m value very small compared with those found for the very good substrate ABTS, indicative that NO was a poor reducing substrate for ELP. As previously reported [14], when native ELP was incubated for 10 min in the presence of 10 mM calcium ions, an activation was observed toward the reducing substrate ABTS, strongly pH-dependent: 100-fold at pH 5.75 and 2-fold activation at pH 7.0. Unexpectedly, at pH 7.0 and in the presence of 10 mM calcium ions, using NO as second substrate, no increase of ELP activity was observed. All kinetic parameters are reported in Table 1.

Table 1
Kinetic parameters of^{2+} ions. Buffer used: 100 mM Tris–HCl, pH 7.0.

	K_m	k_{cat} (s^{-1})	k_{cat}/K_m
ELP			
ABTS [a]	0.55 ± 0.02 mM	170 ± 11	309 mM^{-1} s^{-1}
H_2O_2 [b]	0.12 ± 0.02 mM		1417 mM^{-1} s^{-1}
NO [c]	2.0 ± 0.2 μM	1.1 ± 0.1	0.55 μM s^{-1}
H_2O_2 [d]	1.6 ± 0.1 μM		0.69 μM s^{-1}
ELP-Ca^{2+}			
ABTS [a]	0.41 ± 0.02 mM	270 ± 21	658 mM^{-1} s^{-1}
H_2O_2 [b]	0.074 ± 0.005 mM		3649 mM^{-1} s^{-1}
NO [c]	2.0 ± 0.2 μM	0.8 ± 0.1	0.40 μM s^{-1}
H_2O_2 [d]	1.7 ± 0.2 μM		0.47 μM s^{-1}

[a] Using saturating concentrations of H_2O_2 (25 mM).
[b] Using saturating concentrations of ABTS (10 mM).
[c] Using 10 μM H_2O_2 concentration.
[d] Using 5 μM NO concentration.

3.2. Competitive inhibition mechanism by NO and hydrogen peroxide on the active site of ELP

It is well known that NO inhibits the peroxidase activity [25]. Indeed, as described below, NO binds to the ELP-Fe^{III} forming a stable ferrous nitrosyl complex. Thus, NO competes with hydrogen peroxide. To determine the constant of inhibition (K_i) we calculated the inhibition varying the amount of hydrogen peroxide at fixed concentrations of NO, in the presence and absence of 10 mM Ca^{2+} ions. Since ABTS spontaneously reacts with NO (the oxidation of ABTS occurring at 1:1 stoichiometry with NO [26]), guaiacol was used as second substrate and the initial velocity was determined monitoring the absorption change at 470 nm. We obtained a competitive inhibition with a K_i value, determined by Dixon's plot, of 15.7 (± 1.1) μM. In the presence of calcium ions a higher K_i value was obtained (300 (± 21) μM; not shown).

3.3. Euphorbia peroxidase (ELP-Fe^{III})–NO complex: spectrophotometric features and stopped flow spectroscopy

The electronic absorption spectrum of native ferric ELP, in 100 mM Tris–HCl buffer, pH 7.0, in the presence or in the absence of 10 mM Ca^{2+} ions, showed maxima at 278, 401, 498, and 637 nm (Fig. 2). Both in the absence and in the presence of calcium added and in anaerobic conditions, NO induced an increase and a red shift of the Soret band from 401 to 418 nm. Moreover, two well defined peaks at 530 and 565 nm appeared. These spectral features are very similar to those previously reported for HRP [27], and the shape and positions of these bands are typical of low spin ferrous derivative (ELP-Fe^{II}–NO^+). No further spectral changes were observed after 30 min under anaerobic conditions. After readmission of oxygen, the formation of the original native ELP was observed.

Stopped-flow experiments were used to determine the association (k_{on}) and the dissociation (k_{off}) rates of NO binding to the native ELP in the absence or in the presence of 10 mM Ca^{2+} ions. Experiments were carried out under anaerobic conditions by rapid mixing of a native ELP solution with 100 mM Tris–HCl buffer, pH 7.0, containing different NO concentrations. The formation of the ELP-Fe^{II}–NO^+ complex was monitored following the increase in absorbance at 418 nm. When ferric ELP was mixed with NO, in the absence of calcium, a relatively fast optical change was recorded, leading to a new species identified

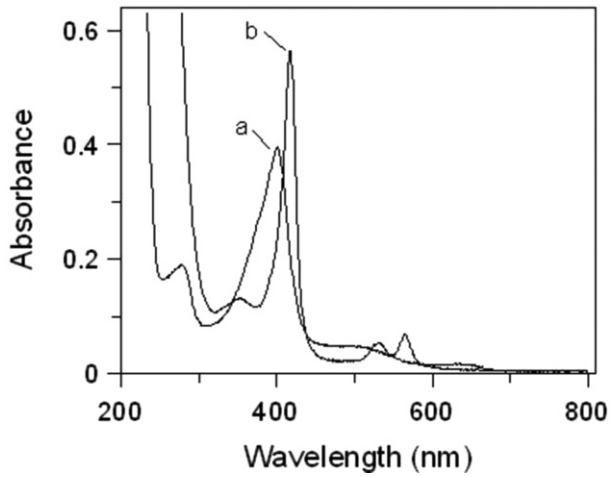

Fig. 2. Electronic absorption spectral change upon NO binding to the ELP-Fe^{III}. (a) ELP native enzyme (3.1 μM) in anaerobic conditions and (b) after addition of NO in excess. Buffer 100 mM Tris–HCl, pH 7.0.

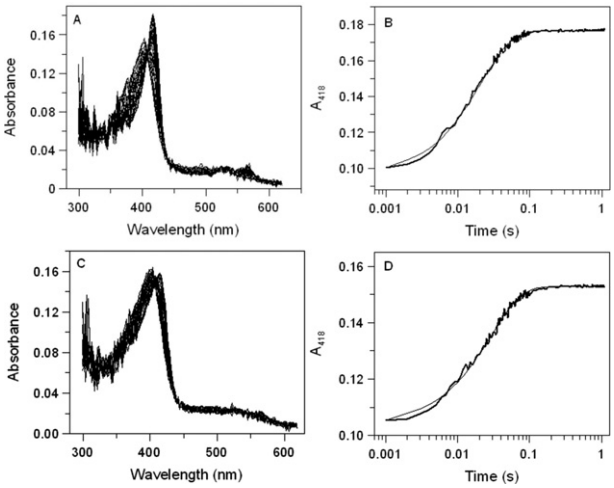

Fig. 3. Time-resolved absorbance spectra recorded after combination of ELP-Fe^{III} with NO. Panel A: time resolved spectra recorded upon mixing 2.3 μM ferric ELP with 40 μM NO (concentrations before mixing). Buffer 100 mM Tris–HCl, pH 7.0; $T = 25$ °C. Panel B: time course at 418 nm extracted from the data reported in Panel A. Panel C: as in Panel A but in the presence of 10 mM $CaCl_2$. Panel D: time course at 418 nm extracted from the data reported in Panel C.

as the complex ELP-Fe^{II}–NO^+ (Fig. 3). The process was clearly reversible since the amplitude of the optical density change depended on the concentration of NO. The rate constants of the combination and dissociation processes, as estimated from a plot of the apparent rate constant versus NO concentration, were 1.50 (± 0.19) × 10^6 M^{-1} s^{-1} for the second order combination and 16 (± 2) s^{-1} for the first order dissociation of the NO complex respectively. The ratio of these rate constants yielded an estimated equilibrium constant of 10 μM (for the dissociation of the ELP^{II}–NO^+ complex), a value which is fully consistent with the K_i reported above. The equilibrium was reached in 0.1 s and no further changes have been observed over 1 s. The plot of the apparent rate constants as a function of NO concentration was linear (not shown), consistent with NO binding in a simple one-step mechanism.

When the same experiment was repeated in the presence of 10 mM calcium ions an essentially similar picture was obtained but the rate and equilibrium constants changed to 0.71 (± 0.11) × 10^6 M^{-1} s^{-1}, 22 (± 2) s^{-1} and 31 μM respectively. According to these estimates, calcium lowers the affinity of ferric ELP for NO by a factor of 3.

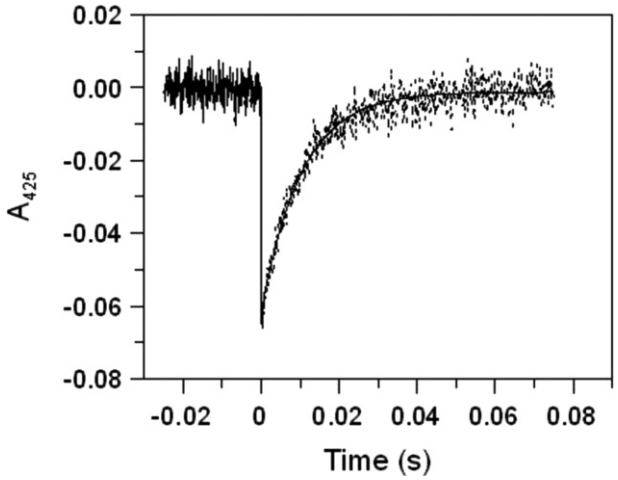

Fig. 4. Laser photolysis of ELP-Fe^{III} with NO. Time course of NO rebinding to ferric ELP after photolysis. Experimental conditions: 8 μM ELP, buffer 100 mM Tris–HCl, pH 7.0, $T = 25$ °C, observation wavelength 425 nm.

This dissociation constant is much lower than the K_i observed, consistent with the higher reactivity of ELP with H_2O_2 that is induced by calcium ions [14].

Since the ELP–NO complex is photolabile, the time course of rebinding could also be recorded by flash photolysis using a pulsed laser source for photoexcitation (Fig. 4). The apparent second order rate constants, recorded by this technique in the presence and in the absence of calcium ions, are very similar (1.15 (± 0.2) × 10^6 M^{-1} s^{-1} in the absence of calcium and 0.9 (± 0.15) × 10^6 M^{-1} s^{-1} in its presence).

However, it is interesting to compare the stopped flow data with the empirical and semi-quantitative observation that O_2 converts ELP–NO to ELP at a slower rate if calcium is present. Indeed, if the reaction was simply due to the consumption of free NO by O_2, it should be slower in the absence of calcium ions and faster in its presence, given that these ions lower the affinity of ELP for NO and speed up the dissociation of the complex. Thus, we take this observation as an indication that NO bound to ELP is more prone to react with O_2 and other substances than free NO in solution. Further observations in this direction are reported below.

3.4. Reaction of ELP with hydrogen peroxide and nitric oxide: spectrophotometric features and stopped flow spectroscopy

The addition of equimolar amount of hydrogen peroxide to native ELP, both in the absence and in the presence of 10 mM Ca^{2+} ions, led to the formation of the Compound I, with characteristic absorption maxima at 278, 398, and 651 nm. In the absence of these ions the addition of DEA/NO to the reaction mixture reduced Compound I to Compound II with characteristic absorption maxima at 278, 417, 522 and 555 nm (Fig. 5). Afterwards, Compound II was reduced to the native enzyme after addition of equimolar amount of DEA/NO.

Although it is not easy to determine the relevant concentration of NO when this gas has been released from DEA/NO, repeated experiments, varying concentrations of ELP (2–4 μM) and/or varying concentrations of DEA/NO, showed that two mol of NO were required to reduce Compound I to the native enzyme (considering 16 min the half-life of DEA/NO and 1.5 the efficiency of NO release; see Section 2). Thus, NO reacted with the oxidised states of the enzyme (Compounds I and II) as an usual substrate (Fig. 6). In the presence of calcium added, after addition of NO to Compound I, we observed a progressive disappearance of the Compound I absorption spectrum, and the gradual formation of the characteristic spectrum of ELP-Fe^{II}–NO^+ complex (not shown). It may be indicative of a slow process

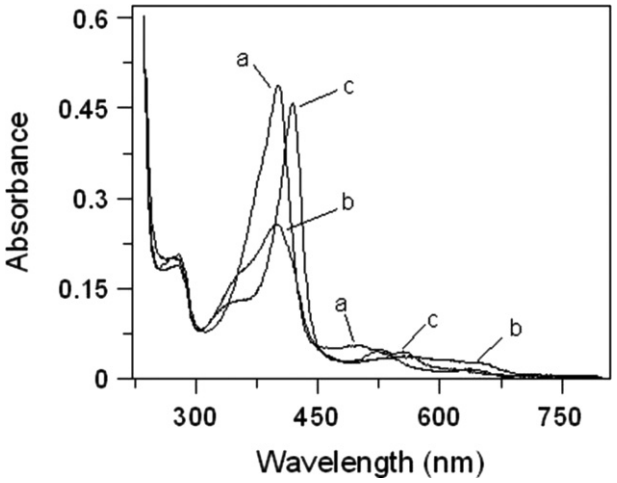

Fig. 5. Absorption spectra of *Euphorbia* peroxidase. (a) ELP native enzyme (3.7 μM); (b) Compound I is formed after addition of equimolar amount of hydrogen peroxide to the native enzyme. (c) Compound II is formed after addition of approximately 3.7 nmol NO to Compound I. Addition of another amount of NO reduced Compound II to the native enzyme. Buffer 100 mM Tris–HCl, pH 7.0.

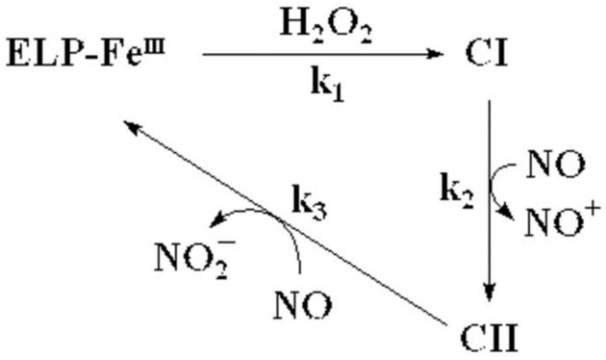

Fig. 6. Kinetic pathway of ELP reacting with hydrogen peroxide and NO as substrates. Compound I is formed after addition of equimolar amount of hydrogen peroxide to the native enzyme. Compound II is formed after addition of equimolar amount of NO generating NO^+. Addition of another equimolar amount of NO reduced Compound II to the native enzyme probably releasing NO_2^-.

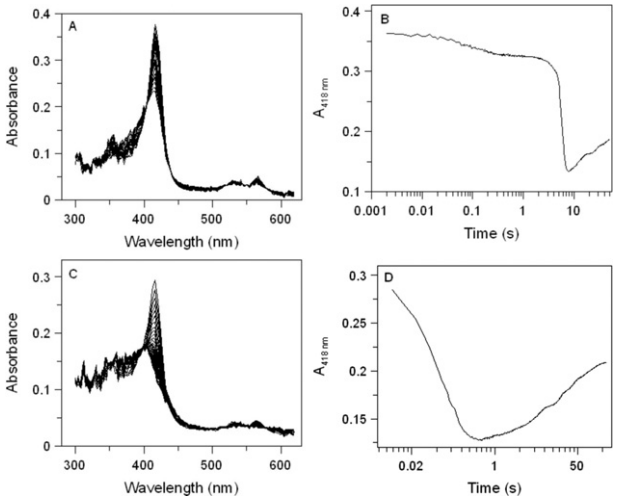

Fig. 7. Time-resolved absorbance spectra recorded after mixing ELP-Fe^{III}–NO with H_2O_2. Panel A: Absorbance spectra recorded after mixing a 3.7 μM solution of ELP, in 100 mM Tris–HCl buffer, pH 7.0, $T = 25$ °C, containing 100 μM NO with a 200 μM solution of H_2O_2, in the absence of calcium ions. Panel B: time course of the experiment in Panel A at 418 nm; notice that release of bound NO is required before the steady state starts. The end of the steady state is marked by the appearance of Compound I, coupled to a very significant decrease of absorbance. The final absorbance increase is presumably due to the partial conversion of Compound I to Compound II caused by H_2O_2 itself. Panel C: experiment as in Panel A, but in the presence of 10 mM $CaCl_2$. Panel D: time course of the experiment as in Panel C at 418 nm. The much faster appearance of Compound I in the presence of calcium (compared with Panel B) is due to the fact that under these experimental conditions the reaction of ELP with H_2O_2 is much faster and thus the steady state mixture is dominated by Compound I, which would be virtually absent in the absence of the cation.

that populates contemporarily several intermediates (Compound I, Compound II, native ELP, and ELP-Fe^{II}–NO$^+$ complex).

The catalytic cycle of ELP with NO and H_2O_2 was also followed by stopped flow experiments. However, due to the properties of the reducing substrate, the experiment had some inherent complexities demanding consideration. A straightforward experiment would be realised by mixing ELP-Fe^{III} with a solution containing NO and H_2O_2 in the desired amounts. However, the long incubation of the two substrates in the driving syringe of the instrument seemed unsafe given the reactivity of both of them. Thus we resorted to two different designs: we either mixed a solution of ELP-Fe^{III} and NO with H_2O_2 or we mixed a solution of Compound I with NO in the presence of minimal excess of H_2O_2. In the former case the actual starting material was the ELP-Fe^{II}– NO$^+$ complex, and dissociation of NO rate limited the onset of the steady state condition. The observed time courses were compatible with the rate constant for NO dissociation from ELP-Fe^{III} measured in the absence of H_2O_2 (see above). The time courses recorded in the absence of calcium (Fig. 7(A)) strikingly differed from those recorded in the presence of this ion (Fig. 7(C)). This result was expected and fully explained by the fact that the reaction of ferric ELP with H_2O_2 is faster in the presence of calcium added [14]. Thus, NO competed very efficiently with H_2O_2 if calcium was absent (Fig. 7(B)) and poorly if this ion was present (Fig. 7(D)). The same reason also explains why, under steady state conditions, the Compound I was more populated in the presence of calcium than in its absence.

In the latter type of experiment, the starting material was Compound I, which, contrary to the ELP-Fe^{II}–NO$^+$ complex, is an intermediate of the ELP catalytic cycle. In single turnover experiments, realised by rapidly mixing Compound I with excess NO, the presence or absence of calcium ions induced striking differences in the time courses. The case of the experiment carried out in the absence of calcium ions was relatively straightforward (Figs. 8(A) and 7(B)). The Compound I had the lowest absorbance at 418 nm and evolved in two subsequent exponential steps, assigned to the formation of Compound II and ELP-Fe^{II}–NO$^+$. We determined the second order rate constant for the transfer of the first electron from NO to the oxidised enzyme, which resulted $2.0(\pm 0.2) \times 10^6\ M^{-1}s^{-1}$. The reaction product, the Compound II, evolved to the ELP-Fe^{II}–NO$^+$ complex in a much slower process that, under our experimental conditions, appeared to be first order with a rate constant of approximately 1 s^{-1}. Only at concentrations of NO lower than its equilibrium constant the reaction rate slowed down and the absorbance change diminished, due to the incomplete saturation of ferric ELP with the gas. In this case the absorbance spectrum at the end of the reaction was consistent with a mixture of ELP-Fe^{III} and ELP-Fe^{II}–NO$^+$ complex. We cannot at present provide a complete explanation of this behaviour but we remark that the observed kinetic process must involve at least two bimolecular processes (one requiring a molecule of NO converting Compound II to the ferric enzyme, the other requiring a further molecule of NO to convert the ferric enzyme to its NO complex) plus one not yet identified monomolecular one.

In the presence of calcium ions (Fig. 8(C) and (D)) the experiment yielded a somewhat more complex time course, since the Compound I present before mixing was not completely converted to Compound II and then to ELP-Fe^{II}–NO$^+$, as we expected. Probably, under these experimental conditions, a side reaction occurred, accounting for the (temporary) loss of a fraction of the molecules of the enzyme, that

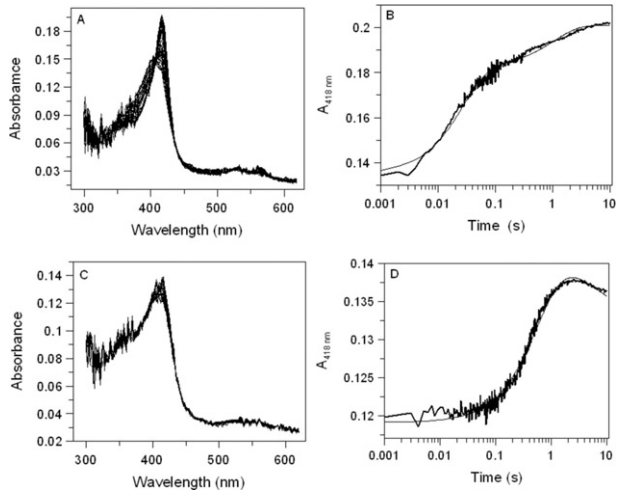

Fig. 8. Time-resolved absorbance spectra recorded after mixing Compound I with excess NO. Panel A: absorbance spectra recorded after mixing a 3.7 μM solution of the Compound I of ELP (obtained by addition to the native enzyme of 3 μM H_2O_2) with 25 μM NO, in 100 mM Tris–HCl buffer, pH 7.0, $T = 25$ °C, in the absence of calcium ions. Panel B: time course of the experiment in Panel A at 418 nm; the continuous line is the result of fitting the data to two sequential exponential decays (see text). Panel C: experiment as in Panel A, but in the presence of 10 mM $CaCl_2$. Panel D: time course of the experiment in Panel C at 418 nm.

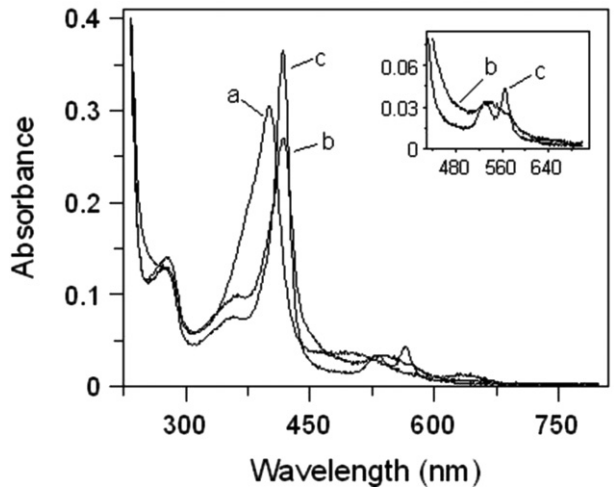

Fig. 9. Absorption spectra of *Euphorbia* peroxidase in the presence of CN^-. (a) Native peroxidase (2.4 μM) in anaerobic conditions; (b) as (a) in the presence of 15 μM CN^-. (c) Addition of an excess of NO to (b). Readmission of oxygen causes the gradually formation of the native enzyme. Inset: expanded absorption visible spectrum showing the differences between (b) and (c).

was recovered over a time regime longer than that explored in our stopped flow measurements.

3.5. Formation of the cyanide derivative: spectrophotometric features of ELP in the presence of CN^- and NO

CN^- behaves as a competitive inhibitor of ELP since it combines with the ferric heme iron. In 100 mM Tris–HCl buffer, pH 7.0, a K_i value of 1.7 ($\pm$ 0.2) $\times$ 10^{-3} M was determined by Dixon's plot, using ABTS and H_2O_2 as substrates. When CN^- was added to ELP, the absorption band at 401 nm disappeared in parallel with formation of a band at 418 nm, and a new peak at 535 nm appeared. The final spectrum obtained is typical of low-spin derivative six-coordinate inactive complex (Fig. 9).

When an excess of NO was added, in anaerobic conditions, to the ELP–CN^- complex, its spectrum immediately changed and the characteristic spectrum of ELP-Fe^{II}–NO^+ complex appeared. No further spectral changes were seen after 3 h in anaerobic conditions indicating that this complex is very stable. Readmission of oxygen caused the gradual formation of the native enzyme (Fig. 9) instead of the expected ELP–CN^- complex, suggesting that cyanide had been consumed in a reaction that involves ELP and NO.

In a successive experiment, even in anaerobic conditions, we added NO to the ELP–CN^- complex in a stoichiometric ratio NO:CN 1:5. Again, the spectrum of the complex immediately changed and the characteristic spectrum of ELP-Fe^{II}–NO^+ complex appeared. This spectrum gradually disappeared after readmission of oxygen with the contemporary formation of the ELP–CN^- spectrum (not shown).

4. Discussion

Studying the extent of NO binding and its oxidation by *Euphorbia* peroxidase, the most interesting and new result is the competition between NO and CN^- for ELP-Fe^{III}, the NO switching off the CN^- from Fe^{III} of ELP in anaerobic condition and the ELP-Fe^{II}–NO^+ complex degraded by cyanide in aerobic conditions.

When considering this reaction mechanism, two important questions arise: (i) how cyanide can react with NO complexed whit ELP (since free CN^- does not react in any case with free NO), and (ii) what could be the reaction products and the role of oxygen. The first question can be answered suggesting that the NO complexed with ELP is more liable to degradation by CN^- than free NO. This is not surprising because, as reported in stopped-flow experiments, we have indications that NO bound to ELP is more prone to react with O_2 and other substances than free NO in solution. For the explanation of the second question, the above reported results induced us to hypothesise a reaction mechanism that operates when ELP is incubated with CN^- and NO. We hypothesise that CN^- reacts with NO forming an unstable transient complex nitrosyl cyanide (ONCN). The formation of this complex has been well described [28]. The solvolysis of nitrosyl cyanide was expected to form, as the hydrolysis products, CO_2 and NH_3 effectively scavenging equimolar amounts of NO and CN^-. Due to the difficulty to detect CO_2 in aqueous solution of this complex environment, we searched ammonia as one of the reaction product which was determined from the amount of NADH consumed in the presence of glutamate dehydrogenase and oxoglutaric acid. At the end of the reaction, 1 mol ammonia/mol CN^- was detected, thus supporting our hypothesis.

Thus, the formation of ONCN from cyanide and NO is a redox reaction that is expected to release an electron. Thus, it cannot proceed in the absence of an oxidant (i.e. under strictly anaerobic conditions), and the role played by oxygen would be that of an electron acceptor.

The above reported mechanism between ELP, NO and CN^- leads us to take in account *in vivo* for the *in vitro* observed modulation of ELP activity. As reported [20], CN^-, formed from the oxidation of the pseudohalide thiocyanate (SCN^-) by ELP in the presence of H_2O_2 and Ca^{2+} ions, reacts with ELP and blocks the enzyme activity. It is plausible that NO levels, increasing in particular conditions, can protect ELP from the inactivation caused by CN^- finely modulating the release of the reaction products.

Besides the main conclusion above reported, several other conclusions are immediately obvious from the experimental findings. NO behaves a substrate for ELP with a very high affinity as detected by experiments with a NO-selective electrode.

The kinetic model for ELP catalysis when NO is used as a second substrate, described in Fig. 6, is compatible with stopped flow and flash photolysis data, but is probably insufficient to describe the complete reaction cycle. Indeed, as one may easily remark, the model predicts inhibition by one of the two substrates (NO). This is compatible with kinetic data but has never been observed in steady state measurements. It is therefore likely that some hitherto uncharacterised

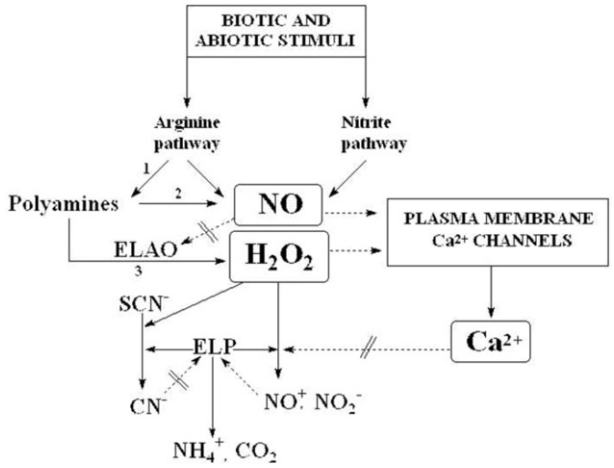

Fig. 10. A variety of biotic and abiotic stresses may elicit the transient increase of NO by both nitrite or arginine pathways. Polyamines, derived from arginine by arginase and arginine decarboxylase (1 in the figure), can increase the NO amount (2 in the figure) [6]. NO can regulate calcium homeostasis by activation of plasma membrane Ca^{2+}-permeable channels [34,35]. The cellular metabolism of polyamines catalysed by *Euphorbia* amine oxidase (ELAO) generates dialdehydes and H_2O_2 [30]. Scavenging of H_2O_2 is mediated by a complex network of enzymes, including ELP which can utilise NO as e second substrate generating H_2O, NO^+ and NO_2^-. H_2O_2 also activates plasma membrane Ca^{2+} channels. Calcium ions, normally necessary for expression of the full activity of the enzyme, inhibit ELP activity in the presence of NO or SCN^- as second substrates. CN^-, obtained by thiocyanate oxidation [20], acts as a reversible inhibitor of ELP and NO switches off the CN^- inhibitory effect (present paper). NO is an irreversible inhibitor of ELAO [36]. Dashed lines mark positive regulations, dashed lines blocked negative ones. Neither all the reaction products nor the reaction stoichiometries are showed in the figure.

chemical reaction may occur, and should be added to the model, causing degradation of bound NO (e.g. ELP-Fe^{II}–NO^+ + H_2O_2 → ELP-Fe^{III} + NO_2 + H_2O). The hypothesis that coordination of NO to the heme iron increases its reactivity towards an oxidant such as H_2O_2 is not unlikely and a similar effect has been observed in cytochrome oxidase and its model compounds for Cu-bound NO [29].

The experiments carried out by stopped flow apparatus do not allow a full description of the steady state oxidation of NO, since the rate constant of conversion of Compound II to ELP could not be precisely determined. However, the rate constants measured in this and preceding works [14], compatible with the Michaelis plots recorded potentiometrically, provided that the second order constant for the reaction of Compound II with NO (k_3 in Fig. 6) is not lower than 5–10 × 10^4 M^{-1} s^{-1}; e.g. simulations carried out with $k_3 = 3 \times 10^5$ M^{-1} s^{-1} yields K_m H_2O_2 = 1.5 μM (to be compared with the experimental value of 1.6 μM reported in Table 1). The agreement between steady state and stopped flow experiments is therefore reasonable, the main discrepantly being that in the simulated plots some substrate inhibition is predicted, which is not observed experimentally. Further work is required to clarify this point.

E. characias latex could represent an interesting experimental model to study the complexity of plant latex biochemistry considering the scheme of multi-enzymatic interactions taking place in this system. Very little information is available about Ca^{2+} signalling, NO production and its metabolism, and H_2O_2 cycling in *Euphorbia* latex and on the associated enzymes. There are evidences clearly indicating the coexistence of multiple enzymatic activities within the latex-driving system of *E. characias* involved in NO and H_2O_2 regulation. We have characterised two main players in this experimental model, namely the H_2O_2-producing amine oxidase (ELAO) [30] – a copper/quinone-containing enzyme that catalyse the oxidative deamination of diamines and polyamines to aldehyde and ammonia – and a Ca^{2+}-regulated Class III secreted peroxidase (ELP), both probably involved in the activation of plant defence responses and in the homeostasis of H_2O_2. Moreover, the two enzymes are believed to be implicated in the oxidative burst through the production of H_2O_2 [31–33]. Thus, based on the results reported here, we propose a model of the interplay between NO, Ca^{2+} and H_2O_2 signalling pathways in *E. characias* latex (Fig. 10). Beyond the references cited in this paper on the production and regulation of NO in plants, two papers deserve attention, the polyamine-induced NO synthesis in plant [6] and the production and cross-talk of NO with calcium signalling [34,35]. As depicted in Fig. 10, these findings further extend our view of latex biochemistry and permit to sketch a more detailed map of some of the multi-enzymatic interactions potentially taking place in this unusual environment.

Acknowledgements

This study was partially supported by a grant from Regione Autonoma della Sardegna, Progetti di Ricerca di Base CRP2–22.

References

[1] Del Rìo LA, Corpas FJ, Barroso JB (2004) Nitric oxide and nitric oxide synthase activity in plants. Phytochemistry. 65, 783–792.
[2] Crawford NM (2006) Mechanisms for nitric oxide synthesis in plants. J. Exp. Bot. 57, 471–478.
[3] Arasimowicz M, Floryszal-Wieczorek J (2007) Nitric oxide as a bioactive signalling molecule in plant stress responses. Plant Sci. 172, 876–887.
[4] Almagro L, Gómez Ros LV, Belchi-Navarro S, Bru R, Ros Barceló A, Pedreño MA (2009) Class III peroxidases in plant defence reactions. J. Exp. Bot. 60, 377–390.
[5] Tun NN, Santa-Catarina C, Begum T, Silveira V, Handro W, Floh EIS et al. (2006) Polyamines induce rapid biosynthesis of nitric oxide (NO) in *Arabidopsis thaliana* seedlings. Plant Cell Physiol. 47, 346–354.
[6] Yamasaki H, Cohen MF (2006) NO signal at the crossroads: polyamine-induced nitric oxide synthesis in plants. Trends Plant Sci. 11, 522–524.
[7] Zamocky, M. and Obinger, C. (2010) Molecular phylogeny of heme peroxidase, in: Biocatalysis Based on Heme Peroxidase (Torres, E. and Ayala, M., Eds.), pp. 7–35.
[8] Welinder KG (1992) Superfamily of plant, fungal and bacterial peroxidises. Curr. Opin. Struct. Biol. 2, 388–393.
[9] Passardi F, Theiler G, Zamocky M, Cosio C, Rouhier N, Teixera F et al. (2007) PeroxiBase: the peroxidase database. Phytochemistry. 68, 1605–1611.
[10] Moerschbacher BM (1992) Plant peroxidases: involvement in response to pathogens. In:C Penel, T Gaspar, H Greppin editors. *Plant Peroxidases 1980–1990, Topics and Detailed Literature on Molecular, Biochemical, and Physiological Aspects*. Switzerland: University of Geneva, p.91–99.
[11] Lamb C, Dixon RA (1997) The oxidative burst in plant disease resistance, Annu. Rev. Plant Physiol. Plant Mol. Biol. 48, 251–275.
[12] Blee KA, Jupe SC, Richard G, Zimmerlin A, Davies DR, Bolwell GP (2001) Molecular identification and expression of the peroxidase responsible for the oxidative burst in French bean (*Phaseolus vulgaris* L.) and related members of the gene family. Plant Mol. Biol. 47, 607–620.
[13] Passardi F, Cosio C, Penel C, Dunand C (2005) Peroxidases have more functions than a Swiss army knife. Plant Cell Rep. 24, 255–265.
[14] Medda R, Padiglia A, Longu S, Bellelli A, Arcovito A, Cavallo S et al. (2003) Critical role of Ca^{2+} ions in the reaction mechanism of *Euphorbia characias* peroxidase. Biochemistry. 42, 8909–8918.
[15] Mura A, Medda R, Longu S, Floris G, Rinaldi AC, Padiglia A (2005) A Ca^{2+}/calmodulin-binding peroxidase from *Euphorbia characias* latex: novel aspects of calcium–hydrogen peroxide cross-talk in the regulation of plant defences. Biochemistry. 44, 14120–14130.
[16] Mura A, Longu S, Padiglia A, Rinaldi AC, Floris G, Medda R (2005) Reversible thermal inactivation and conformational states in denaturant guanidinium of a calcium-dependent peroxidase from *Euphorbia characias*. Int. J. Biol. Macromol. 37, 205–211.
[17] Pintus F, Spanò D, Medda R, Floris G (2011) Calcium ions and a secreted peroxidase in *Euphorbia characias* latex are made for each other. Protein J. 30, 115–123.
[18] Mura A, Pintus F, Lai P, Padiglia A, Bellelli A, Floris G et al. (2006) Catalytic pathways of *Euphorbia characias* peroxidase reacting with hydrogen peroxide. Biol. Chem. 387, 559–567.
[19] Mura A, Pintus F, Fais A, Porcu S, Corda M, Spanò D et al. (2008) Tyramine oxidation by copper/TPQ amine oxidase and peroxidase from *Euphorbia characias* latex. Arch. Biochem. Biophys. 475, 18–24.
[20] Pintus F, Spanò D, Bellelli A, Angelucci F, Scorciapino AM, Anedda R et al. (2010) *Euphorbia* peroxidase catalyzes thiocyanate oxidation in two different ways, the distal calcium ion playing an essential role. Biochemistry. 49, 8739–8747.
[21] Keefer LK, Nims RW, Davies KM, Wink DA (1996) "NONOates" (1-substituted diazen-1-ium-1,2-diolates) as nitric oxide donors: convenient nitric oxide dosage forms. Methods Enzymol. 268, 281–293.
[22] Tayefi-Nasrabadi H, Dehghan G, Daeihassani B, Movafegi A, Samadi A (2011) Some biochemical properties of guaiacol peroxidases as modified by salt stress

in leaves of salt-tolerant and salt-sensitive safflower (*Carthamus tinctorius* L.cv.) cultivars. Afr. J. Biotechnol. 10, 751–763.
[23] Wilson EK, Bellelli A, Liberti S, Arese M, Grasso S, Cutruzzola F et al. (1999) Internal electron transfer and structural dynamics of cd_1 nitrite reductase revealed by laser CO photodissociation. Biochemistry. 38, 7556–7564.
[24] Arcovito A, Gianni S, Brunori M, Travaglini Allocatelli C, Bellelli A (2001) Fast coordination changes in cytochrome c do not necessarily imply folding. J. Biol. Chem. 276, 41073–41078.
[25] Abu-Soud HM, Hazen SL (2000) Nitric oxide modulates the catalytic activity of myeloperoxidase. J. Biol. Chem. 275, 5425–5430.
[26] Nims RW, Cook JC, Krishna MC, Christodoulou D, Poore CMB, Miles AM et al. (1996) Colorimetric assays for nitric oxide and nitrogen oxide species formed from nitric oxide stock solutions and donor compounds. Method Enzymol. 268, 93–105.
[27] Qiang L, Zhu S, Ma H, Zhou J (2010) Investigation on binding of nitric oxide to horseradish peroxidise by absorption spectrometry. Spectrochim. Acta A. 75, 417–421.
[28] Shirota FN, Goon DJW, De Master EG, Nagasawa HT (1996) Nitrosyl cyanide, a putative metabolic oxidation product of the alcohol-deterrent agent cyanamide. Biochem. Pharmacol. 52, 141–147.
[29] Aguirre E, Rodrìguez-Juàrez F, Bellelli A, Gnaiger E, Cadenas S (2010) Kinetic model of the inhibition of respiration by endogenous nitric oxide in intact cells. Biochim. Biophys. Acta. 1797, 557–565.
[30] Padiglia A, Medda R, Lorrai A, Murgia B, Pedersen JZ, Finazzi Agrò A et al. (1998) Characterization of *Euphorbia characias* latex amine oxidase. Plant Physiol. 117, 1363–1371.
[31] Mittler R, Vanderauwera S, Gollery M, Van Breusegem F (2004) The reactive oxygen gene network of plants. Trends Plant Sci. 9, 490–498.
[32] Medda R, Padiglia A, Floris G (1995) Plant copper-amine oxidases. Phytochemistry. 39, 1–9.
[33] Laurenzi M, Tipping AJ, Marcus SE, Knox JP, Federico R, Angelini R et al. (2001) Analysis of the distribution of copper amine oxidase in cell walls of legume seedlings. Planta. 214, 37–45.
[34] Lamotte O, Courtois C, Dobrowolska G, Besson A, Pugin A, Wendehenne D (2006) Mechanisms of nitric-oxide-induced increase of free cytosolic Ca^{2+} concentration in *Nicotiana plumbaginifolia* cells. Free Radical Biol. Med. 40, 1369–1376.
[35] Besson-Bard A, Courtois C, Gauthier A, Dahan J, Dobrowolska G, Jeandrozc S et al. (2008) Nitric oxide in plants: production and cross-talk with Ca^{2+} signalling. Mol. Plant. 1, 218–228.
[36] Longu S, Padiglia A, Pedersen JZ, Finazzi Agrò A, Mura A, Maccioni P et al. (2005) Nitric oxide covalently labels 6-hydroxydopa-derived free radical intermediate in the catalytic cycle of copper/quinone containing amine oxidase from lentil seedlings. Biol. Chem. 386, 25–31.